

# Stray-fields based features observed for low and high magnetic fields in $\text{Ni}_{80}\text{Fe}_{20}\text{-Nb-Ni}_{80}\text{Fe}_{20}$ trilayers

D. Stamopoulos, \* E. Manios, N. Papachristos and I. Aristomenopoulou

*Institute of Materials Science, NCSR "Demokritos", 153-10, Aghia Paraskevi, Athens, Greece.*

(Dated: November 1, 2018)

In this work we report on the influence of stray fields for both low and high magnetic fields applied parallel to hybrid trilayers that consist of a low- $T_c$  Nb interlayer and of two outer  $\text{Ni}_{80}\text{Fe}_{20}$  layers having in-plane but no uniaxial anisotropy as this is evidenced by complete magnetization data obtained in the normal state. At low magnetic fields these trilayered hybrids exhibit a pronounced magnetoresistance effect. The dynamic transport behavior of the trilayers is presented in the regime of the magnetoresistance effect through detailed I-V characteristics. More importantly, the detailed evolution of the *longitudinal* and *transverse* magnetic components of the trilayers is presented from very close to  $T_c^{SC}$  to well inside the superconducting regime. These data clearly show that below  $T_c^{SC}$  and for low magnetic fields the transport properties of the Nb interlayer are influenced by *transverse* stray-fields that motivate subsequent *transverse* magnetic coupling of the outer  $\text{Ni}_{80}\text{Fe}_{20}$  layers. By generalizing this experimental finding we propose that the generic prerequisite for the occurrence of intense magnetoresistance effects in relative ferromagnetic-superconducting-ferromagnetic trilayers is that the coercive fields of the respective outer layers should almost coincide. Thus, owing to the *simultaneous* occurrence of magnetic domains all over the surface of the ferromagnetic layers these are susceptible to *transverse* magnetic coupling mediated by the accompanying *transverse* stray fields occurring mainly above domain walls. Finally, the behavior of the  $\text{Ni}_{80}\text{Fe}_{20}\text{-Nb-Ni}_{80}\text{Fe}_{20}$  trilayer's upper-critical field is investigated in comparison to Nb- $\text{Ni}_{80}\text{Fe}_{20}$  bilayers and Nb single layers. The trilayer's upper-critical field exhibits a pronounced suppression for low magnetic fields indicative of a *2D* behavior, while for high values the conventional *3D* behavior represented by a linear temperature variation is recovered. A similar process is observed in both the Nb- $\text{Ni}_{80}\text{Fe}_{20}$  bilayer and in the Nb single layer reference films. However, significant qualitative and quantitative differences exist between these samples. Based on a mechanism that is motivated by *longitudinal* stray-fields existing exclusively in the high-field regime we propose a possible interpretation for this experimental finding.

PACS numbers: 74.45.+c, 74.78.Fk, 74.78.Db

## I. INTRODUCTION

Since the discovery of the giant magnetoresistance (GMR) effect<sup>1</sup> trilayers (TLs) comprised of two ferromagnetic (FM) electrodes and a normal metal (NM) interlayer have attracted much interest<sup>2</sup>. Apart from a NM an insulator (IN) may also be used as an interlayer so that the hybrid TL is called tunnel valve and the respective effect tunnel magnetoresistance.<sup>3,4</sup> Recently, relative hybrids consisting of superconducting (SC) and FM constituents have attracted much interest both experimentally<sup>5,6,7,8,9,10,11,12,13,14,15,16,17,18</sup> and theoretically.<sup>19,20,21,22,23,24,25</sup> The concept of a superconductive spin valve was theoretically proposed in Refs.24,25. It is based on a FM-SC-FM TL where the nucleation of superconductivity can be controlled by the in-plane *relative* magnetization orientation of the outer FM layers. J.Y. Gu et al.<sup>6</sup> were the first who reported on the experimental realization of a  $[\text{Ni}_{82}\text{Fe}_{18}\text{-Cu}_{0.47}\text{Ni}_{0.53}]/\text{Nb}/[\text{Cu}_{0.47}\text{Ni}_{0.53}\text{-Ni}_{82}\text{Fe}_{18}]$  spin valve. I.C. Moraru et al.<sup>8</sup> also studied a great number of Ni-Nb-

Ni TLs and observed a significantly larger shift of the superconducting transition temperature  $T_c^{SC}$  than that reported in Refs.6,7. In these works<sup>6,7,8</sup> the exchange bias was employed in order to "pin" the magnetization of the one FM layer and it was observed that when the magnetizations of the two FM layers were parallel (antiparallel) the resistive transition of the SC was placed at lower (higher) temperatures. V. Peña et al.<sup>9</sup> and A.Yu. Rusanov et al.<sup>10</sup>, studied  $\text{La}_{0.7}\text{Ca}_{0.3}\text{MnO}_3\text{-YBa}_2\text{Cu}_3\text{O}_7\text{-La}_{0.7}\text{Ca}_{0.3}\text{MnO}_3$  and  $\text{Ni}_{80}\text{Fe}_{20}\text{-Nb-Ni}_{80}\text{Fe}_{20}$  TLs, respectively and they reported the exact opposite behavior; they observed that when the magnetizations of the two FM layers were parallel (antiparallel) the resistive transition of the SC interlayer was placed at higher (lower) temperatures. In a very recent work of ours<sup>14</sup> that dealt with exchange biased  $\text{Ni}_{80}\text{Fe}_{20}\text{-Nb-Ni}_{80}\text{Fe}_{20}$  TLs we have also derived the same conclusions. Also, C. Visani et al. in Ref.17 confirmed the experimental results of Ref.9 only very recently. In addition, in the work of V. Peña et al.<sup>9</sup> and C. Visani et al.<sup>17</sup> a GMR-like effect was observed that it was related to the occurrence of spin imbalance<sup>26</sup> in the SC, ultimately motivated by the high spin polarization (almost 100%) of  $\text{La}_{0.7}\text{Ca}_{0.3}\text{MnO}_3$ .

Here we present results on stray-fields motivated features for both low and high magnetic fields in TLs constructed of low spin polarized  $\text{Ni}_{80}\text{Fe}_{20}$  and low- $T_c$

\*Author to whom any correspondence should be addressed: densta@ims.demokritos.gr

Nb. These TLs exhibit a pronounced magnetoresistance (MR) effect ( $\Delta R/R_{nor} \times 100\% = 45\%$ ) in the low-field regime.<sup>27</sup> Their dynamic transport behavior is presented through detailed I-V characteristics. These TLs are plain, in the sense that don't incorporate the mechanism of exchange bias as the ones studied in Ref.14. Specifically, we present the complete magnetic characterization of the TLs that they exhibit in-plane but no uniaxial anisotropy. More importantly, detailed magnetization measurements of both the *longitudinal* and *transverse* magnetic components that are performed from very close to well below  $T_c^{SC}$  reveal the complete evolution of a magnetostatic coupling of the outer  $Ni_{80}Fe_{20}$  layers that forces the Nb interlayer to attain a magnetization component *transverse* to the external magnetic field. These magnetic characteristics are cornerstones for the explanation of the observed MR effect since they prove that this is motivated by a *transverse* magnetic interconnection of the outer  $Ni_{80}Fe_{20}$  layers through *transverse* stray fields that emerge near coercivity. Ultimately, these *transverse* stray fields locally amount to the lower or even the upper critical field of the Nb interlayer so that they suppress its transport properties.

By generalizing our experimental findings we propose a generic *transverse* stray-fields mechanism that could assist us toward the explanation of the contradictory experimental results that have been reported in the recent literature regarding the transport properties of relevant FM-SC-FM TLs.<sup>6,7,8,9,10,11,12,13,14,15,16,17</sup> According to this proposal the generic prerequisite for the occurrence of intense MR effects is that the coercive fields of the respective outer FM layers should almost be the same. When this condition is fulfilled, the two FM layers are susceptible to *transverse* magnetic coupling that is efficiently mediated by the *transverse* stray fields accompanying the magnetic domain walls that emerge *simultaneously* all over the surface of the FM layers around their nearly common coercivity.

Finally, the behavior of the TL's upper-critical field is investigated in comparison to the respective ones of a SC-FM bilayer (BL) and a SC single layer (SL) reference films. The TL's upper-critical field,  $H_{c2}^{SC}(T)$  exhibits an intense crossover from two-dimensional (2D) to three-dimensional (3D) behavior when compared to the BL and the SL. This is exhibited by a pronounced rounding observed in the  $H_{c2}^{SC}(T)$  curve for low magnetic fields, while for high values the conventional linear temperature variation is recovered. Since for high magnetic fields the two FM layers are saturated possible *transverse* stray fields located above domain walls are minimized and only *longitudinal* ones that run along their surfaces are mainly present. Based on a *longitudinal* stray-fields mechanism we propose a possible interpretation for this experimental feature.

## II. PREPARATION AND CHARACTERIZATION OF SAMPLES. EXPERIMENTAL DETAILS

The samples were sputtered on Si [001] substrates under an Ar environment (99.999% pure). In order to eliminate the residual oxygen that possibly existed in the chamber we performed Nb pre-sputtering for very long times since Nb acts as a strong oxygen getter.<sup>13,28,29</sup> The Nb layers were deposited by dc-sputtering at 46 W and an Ar pressure of 3 mTorr,<sup>13,28,29</sup> while for the  $Ni_{80}Fe_{20}$  (NiFe) layers rf-sputtering was employed at 30 W and 4 mTorr. In this work we show detailed results for NiFe(19)-Nb(50)-NiFe(38) TLs (in nanometer units). Quantitatively, the same results were obtained for NiFe(19)-Nb(50)-NiFe(19) ones. We should stress that: (i) all depositions were carried out *at room temperature* and (ii) *no* external magnetic field was applied during the deposition of the NiFe layers. However, the samples can't be shielded from the residual magnetic fields (of the order 10 – 15 Oe) existing in the chamber of our sputtering unit. Thus, our NiFe films exhibit in-plane anisotropy. However, they don't exhibit uniaxial anisotropy since the magnetic field sources are placed symmetrically on the perimeter of the circular rf-gun. The produced NiFe films have low coercive fields of order 10 Oe. The critical temperature of the TLs studied in this work is  $T_c^{SC} \approx 7.4$  K. These characteristics are shown in figures 1(a) and 1(b) where the *longitudinal* magnetic component is presented for cases where the external magnetic field was applied either parallel or normal to the TL.

Our MR measurements were performed by applying a dc-transport current ( $I_{dc} = 0.5$  mA, always normal to the magnetic field) and measuring the voltage in the standard four-point straight configuration. The temperature control and the application of the magnetic fields were achieved in a superconducting quantum interference device (SQUID) (Quantum Design). In most cases presented in this work the applied field was parallel to the films. Cases where it was applied normal will be specified explicitly.

## III. TRANSPORT DATA

As may be seen in figure 2(a) the zero-field critical temperature of the TL is  $T_c^{SC} = 7.42$  K. This value is very close to the one that is magnetically determined (see figure 1(b)). Figures 2(b) and 2(c) show the main raw transport results of our work. Presented are detailed voltage curves  $V(H)$  as a function of magnetic field in the normal (panel (b)), and in the superconducting (panel (c)) state at various temperatures across its zero-field resistive curve presented in panel (a). All these data were obtained for the parallel-field configuration. We see that for  $T > T_c^{SC}$  conventional MR is revealed with values 0.6%. In contrast, in the superconducting state the percentage resistance change  $(R_{max} - R_{min})/R_{nor} \times 100\%$

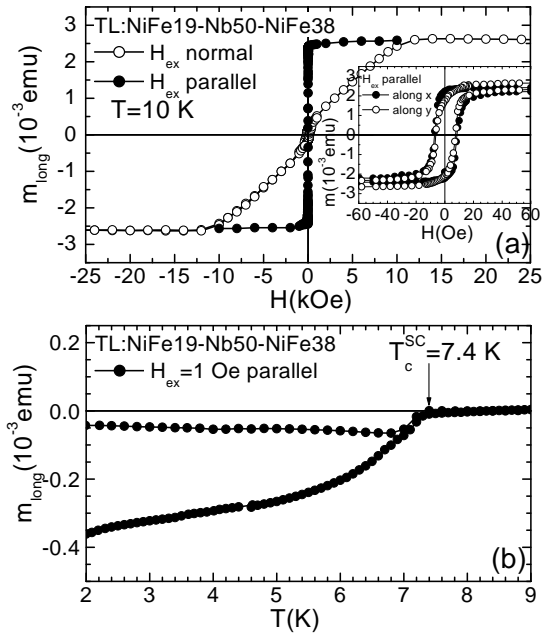


FIG. 1: (Panel (a)) Longitudinal magnetization  $m(H)$  data obtained for a TL at  $T=10\text{ K} > T_c^{SC}$  when the external magnetic field was both parallel (solid circles) and normal (open circles). (Panel (b)) Magnetization  $m(T)$  curve obtained at  $H_{ex} = 5\text{ Oe}$  applied parallel to the same TL for determination of its  $T_c^{SC}$ . The offset owing to the FM layers has been removed. (Inset) The respective  $m(H)$  data shown in the main panel (a) as obtained when the external field was applied along the two in-plane dimensions of the TL.

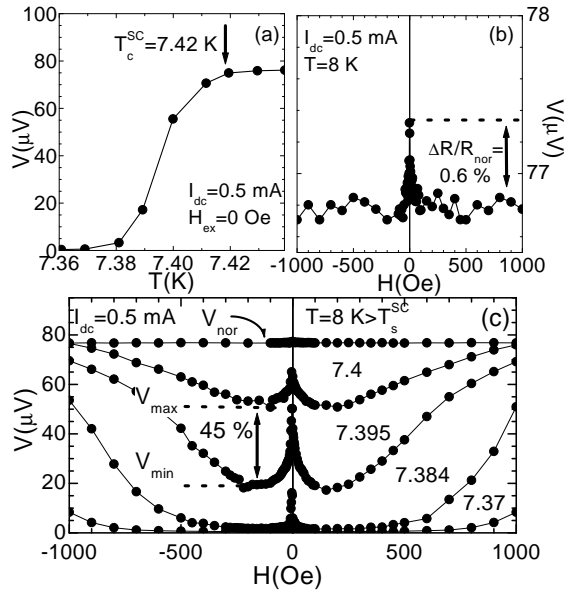


FIG. 2: (Panel (a)) Zero-field resistive curve  $V(T)$  of a TL. (Panel (b))  $V(H)$  curve at  $T=8\text{ K} > T_c^{SC} = 7.42\text{ K}$ . (Panel (c))  $V(H)$  curves at various temperatures across the TL's resistive transition presented in panel (a). In all cases the magnetic field was applied parallel to the TL.

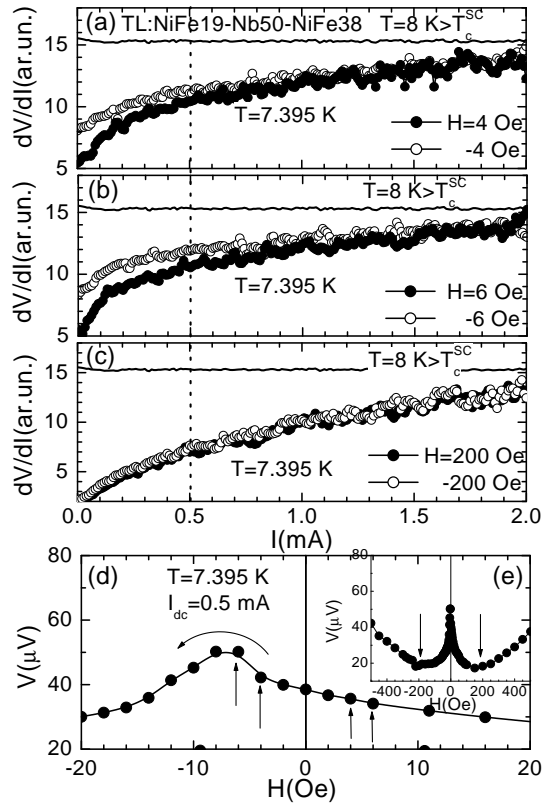


FIG. 3: Representative I-V characteristics obtained at  $T=7.395\text{ K}$  for various magnetic fields ranging from very close to the MR peak (Panel (a)-Panel (b)) to far away (Panel (c)). (Panel (d)) Low-field details of the MR  $V(H)$  curve obtained at  $T=7.395\text{ K}$ . The inset presents an extended field range of the MR curve for clarity. The arrows indicate the exact points where the I-V experiments were performed. In all cases the magnetic field was applied parallel to the TL.

that we observe is 45%.<sup>30</sup> Thus, as we enter the superconducting state the observed *increase is of two orders of magnitude!* This signifies that the mechanisms motivating the MR peaks in the normal and superconducting states of the TL hybrid are surely different. Here we should stress that the pronounced MR effect discussed for the NiFe-Nb-NiFe TLs is not observed in more simple NiFe-Nb bilayers (BLs).<sup>27</sup> In these BLs only a minor effect exists; the respective percentage resistance change  $(R_{max} - R_{min})/R_{nor} \times 100\%$  by no means exceeds 8%. For detailed transport results on the BLs see Ref.27. According to the quantitative criteria the MR effect that we observe in the TLs can be considered as GMR.<sup>9</sup> However, as we show below the main mechanism motivating the observed phenomenon is not related to the usual spin-dependent scattering mechanism motivating the GMR effect.<sup>1,2</sup>

The dynamic behavior of the MR effect is revealed by the I-V characteristics shown in figures 3(a)-3(e). These data were obtained at  $T=7.395\text{ K}$  for the parallel-field configuration. In panels (a)-(b) we present low-field data

around the MR peak, while in panel (c) shown is a representative curve that reveals the behavior for high magnetic fields away from the MR peak's maximum. Low-field details of the respective  $V(H)$  curve are presented in panel (d), while its inset shows an extended field range for clarity. The arrows indicate the exact points where the I-V characteristics were carried out. The dotted vertical line in panels (a)-(c) shows the specific value  $I_{dc} = 0.5$  A of the transport current where the  $V(H)$  curve shown in panel (d) was obtained. From these data we clearly see that for low magnetic fields, i.e. around the MR peak the polarity of the applied field plays a crucial role. In contrast, for high magnetic fields, i.e. away from the MR peak the obtained I-V curves don't depend on field's polarity since they clearly coincide. In addition, even for low magnetic fields the I-V response depends on the transport current. For low applied currents the curves obtained for opposite polarity clearly diverge, while for high applied currents they eventually coincide.

#### IV. MAGNETIZATION DATA

First of all we have to underline that our TLs exhibit a very soft magnetic character of in-plane anisotropy. However, they don't have uniaxial anisotropy so that as coercivity is approached most possibly the magnetization reverses in a non-coherent way; the FM layers segregate into magnetic domains that each one reverses independently from the others. These characteristics are shown in figure 1(a). In the inset we present representative magnetization loops that were obtained while the external magnetic field was applied parallel to the TL and in two different directions along its two basic dimensions. We clearly see that the two loops coincide absolutely exhibiting coercivity of less than 10 Oe. The same behavior was also obtained for other directions where the magnetic field was applied. Thus, we conclude that our hybrid TLs exhibit in-plane but no uniaxial anisotropy. Finally, we have to stress that regarding the in-plane anisotropy we can't distinguish between a component that originates from an intrinsic mechanism and another one that has a shape origin.

In order to investigate the underlying mechanism responsible for the pronounced MR effect we performed detailed magnetization loops for the *longitudinal* and *transverse* magnetic components both well below and above  $T_c^{SC}$ . Representative results are shown in figures 4(a) and 4(b) for the parallel-field configuration. The inset of panel (a) presents the exact configuration of the external field and of each magnetic component, while the one of panel (b) focuses on low-field details of the transverse magnetization curve obtained at  $T = 8$  K  $> T_c^{SC}$ . Let us first discuss panel (a), that is the data referring to the longitudinal component. These data reveal a surprising fact: we see that not only above  $T_c^{SC}$  but even well below  $T_c^{SC}$  the longitudinal component resembles the loop of a FM as if the SC is absent (the only finger-

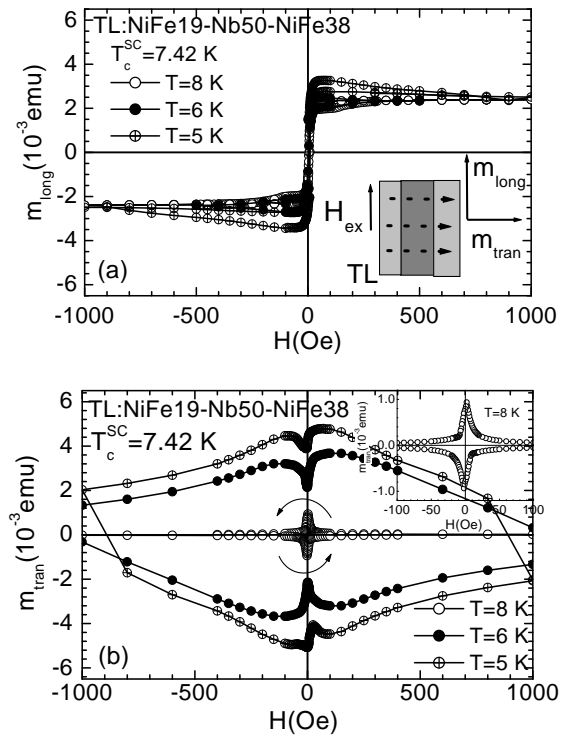


FIG. 4: (Panel (a)) Magnetization  $m(H)$  data referring to the longitudinal magnetic component of a TL obtained both above and well below  $T_c^{SC}$ . (Panel (b)) The respective data for its transverse magnetic component. The inset of panel (a) presents schematically the configuration of the external field and of each magnetic component of the TL, while the respective of panel (b) focuses on low-field details of the transverse magnetization curve obtained in the normal state. In all cases the magnetic field was applied parallel to the TL.

print of its presence comes from the comparatively small irreversibility that shows up below  $T_c^{SC}$ ). This reveals that the outer NiFe layers interact strongly through the Nb interlayer even well inside the superconducting state so that bulk superconductivity is strongly suppressed at least when referring to the longitudinal component. Referring to the transverse component, in panel (b) we see that the normal-state curve attains significant values of the order 35% of the saturated longitudinal one (see the respective inset). This clearly proves that in the normal state a significant part of the TL's magnetization rotates out of plane near zero magnetic field. Proceeding with the data obtained in the superconducting state we stress that they reveal a striking feature: the out-of-plane rotation of the TL's magnetization is not observed only in the normal state but also well inside the superconducting state of Nb. We see that the transverse component of the TL obtains the model loop expected for a SC when the mechanism of bulk pinning of vortices dominates.<sup>31</sup> *The data presented in figure 4 imply that the SC behaves diamagnetically not in respect to the parallel external field but in respect to a new transverse field that emerges ow-*

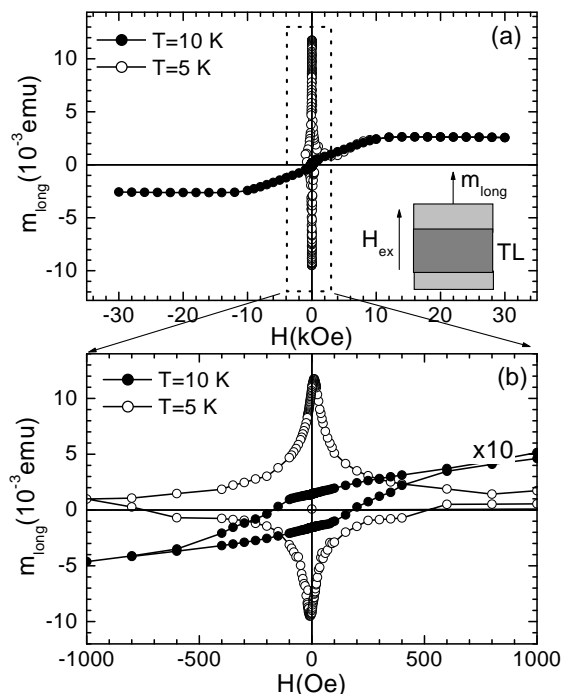


FIG. 5: (Panel (a)) Longitudinal magnetization  $m(H)$  data that were obtained when the magnetic field was applied normal to the TL for both above and well below  $T_c^{SC}$  in an extended field range. (Panel (b)) The respective data focused in the low-field regime. For clarity the curve obtained at  $T=10$  K is multiplied by a factor of 10. The inset of panel (a) presents schematically the configuration between the normal magnetic field and the measured magnetization component.

*ing to the magnetic coupling of the outer NiFe layers as this is schematically presented in the inset of panel (a) by the dotted arrows.*

For the normal-field configuration the obtained results are more conventional. Representative magnetization loops for the *longitudinal* magnetic component for both above and well below  $T_c^{SC}$  for the normal-field configuration are shown in figures 5(a) and 5(b) for high and low values of the magnetic field, respectively. The inset of panel (a) presents schematically the configuration between the normal magnetic field and the longitudinal magnetization component. We clearly see that in this field configuration the magnetization loop that is obtained below  $T_c^{SC}$  resembles the model one expected for a SC when the mechanism of bulk pinning of vortices dominates.<sup>31</sup>

## V. DISCUSSION

### A. Stray-fields *transverse* coupling of the outer FM layers

It is well known that in relevant TLs of non-superconducting interlayer the interaction of the outer FM layers through stray fields that occur at domain walls may lead to significant magnetostatic coupling.<sup>3,4</sup> This behavior is expected to be pronounced when the FM layers have a multidomain magnetic state, that is in the low magnetic field regime near coercivity as this is observed in our FM-SC-FM TLs. S. Parkin and colleagues have shown that such stray-fields coupling that occurs at domain walls plays a unique role in FM-IN-FM and FM-NM-FM TLs.<sup>3,4</sup> Accordingly, in our case the partial out-of-plane rotation of the TL's magnetization that we observe in the normal state (see figure 4(a)), and most importantly *its unique transverse magnetic component that we observe in the superconducting state* (see figure 4(b)) are motivated by such a stray-fields magnetostatic coupling of the outer NiFe layers. We believe that this is the case since the pronounced MR effect is observed around the coercive field where the FM layers segregate in magnetic domains so that a rich reservoir of *transverse* stray fields is available to mediate their magnetic coupling *all over their surface*.

Ultimately, the magnetostatic coupling discussed here could motivate the MR peaks presented in figure 2(c) as follows: the *transverse* stray fields that interconnect the outer NiFe layers penetrate completely the Nb interlayer as this is schematically presented in the inset of figure 4(a) by the dotted arrows. Consequently, in some areas not only the lower but even the upper critical field of the Nb interlayer may be exceeded locally. This should result in a suppression of its superconducting properties for low magnetic fields where this transverse field gets maximum (see figure 4(b)). Indeed, this is evident not only in our MR curves (see figure 2(c)), but also in our transverse magnetization data where clear dips are observed near zero field probably indicating a small suppression of bulk superconductivity (see figure 4(b)). Under a different point of view the data presented in figure 4(b) may be interpreted as following: below  $T_c^{SC}$  the magnetization of the Nb interlayer is *opposite* to the one of the outer NiFe layers, indicating the *diamagnetic* behavior of the SC in respect to the FM layers' transverse magnetization field. In order to show the clear evolution of this effect in figure 6 we present a detailed loop for another TL very close to the  $T_c^{SC}$ . We clearly see that the transverse magnetic component of the SC interlayer is *opposite (diamagnetic)* to the respective of the FM outer layers.

These arguments explains naturally the absence of the pronounced MR effect in the NiFe-Nb BLs that was stated above.<sup>27</sup> Although even in the BLs the magnetization of the single NiFe layer may partially rotate out of plane it doesn't have the opportunity to get coupled with an adjacent NiFe one (as happens in the TLs) so that the

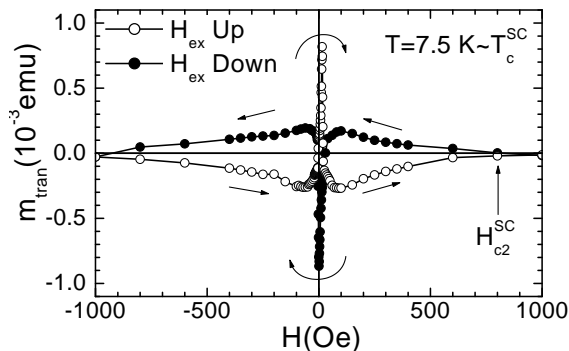


FIG. 6: Complete magnetization  $m(H)$  loop for the transverse magnetic component of a TL obtained just below its  $T_c^{SC}$ .

existing *transverse* stray fields don't penetrate the Nb interlayer completely (see below). As a consequence the MR effect observed in the BLs ( $(R_{max} - R_{min})/R_{nor} \times 100\% = 8\%$ ) is only minor when compared to the one of the TLs ( $(R_{max} - R_{min})/R_{nor} \times 100\% = 45\%$ ).

### B. Comparison with relevant experiments

In this section we compare our results with other experimental works available in the recent literature. First of all let us compare our results with those presented in Ref.10 since both works refer to the same FM and SC constituents. We believe that the specific magnetic characteristics that our films attain owing to the preparation process explain the differences in both the magnitude of the MR (5% – 10% in Ref.10, while 40% – 50% in our work<sup>30</sup>) and the proposed mechanisms between the TLs studied in Ref.10 and in our work. A. Yu. Rusanov et al. reported<sup>10</sup> on the MR of similar NiFe-Nb-NiFe TLs and attributed the MR peaks that they observed to the in-plane antiparallel alignment of the outer NiFe layers. Their samples exhibited strong in-plane uniaxial anisotropy. Thus, in their case as the magnetic field passes through zero the magnetization of each NiFe layer reverses *coherently* and probably entirely in-plane (although data on the transverse magnetic component are not presented in Ref.10). In our case it is surely extreme to invoke that the magnetization of the outer NiFe layers rotates coherently; their very soft magnetic character ensures that as coercivity is approached a rich multidomain magnetic state is attained. Thus, *transverse* stray fields that emerge above domain walls that are spread all over the surface of the FM layers may mediate their magnetic coupling efficiently. Unavoidably, the SC interlayer will be magnetically "pierced".

We stress that the importance of the out-of-plane rotation of the outer FM layers' magnetizations revealed by our results could be relevant in all relative FM-SC hybrids that were studied very recently.<sup>6,7,8,9,10,11,12,13,14,15,16,17</sup> The influence of stray

fields originating from a FM multilayer on an adjacent SC was already highlighted by some of us in Refs.11,12,13. R. Steiner and P. Ziemann revealed the influence that stray fields have on a SC interlayer in their recent work<sup>15</sup> referring to Co-Nb-Fe and CoO-Nb-Fe TLs for the parallel-field configuration. Also, very recently C. Monton et al.<sup>18</sup> studied stray-fields induced effects in Nb/Co multilayers when the magnetic field was applied parallel to their surface and reported a behavior similar to the one observed in Refs.11,12,13. However, C. Monton et al.<sup>18</sup> expanded our knowledge to the complete mutual effect; the authors<sup>18</sup> revealed convincingly that the screening coming from the SC layers influences drastically the magnetic domain state of the adjacent FM ones. In contrast, A Singh et al. in Ref.16 studied in the normal-field configuration Co-Pt/Nb/Co-Pt TLs of perpendicular magnetic anisotropy and claimed that stray fields don't actually influence the SC interlayer. This interpretation was based on experimental data that were obtained when an insulating SiO<sub>2</sub> layer was introduced at each Co-Pt/Nb interface so that the electronic coupling of the two constituents was removed. However, in the specific transport experiments that were presented in Ref.16 each FM layer was in its saturated magnetic state so that possible stray fields were only limited at the specimen's edges.

Here, we present uncontested evidence for the dominant influence of *transverse* stray-fields coupling of the outer NiFe layers on the Nb interlayer in the respective TLs (see also Ref.27). We have to stress that in our work we refer not to the stray fields that exist *only near the edges* of a homogeneously magnetized FM as it was discussed in Ref.16 but to the *transverse* stray fields that emerge naturally *all over the surface* of the FM owing to the appearance of magnetic domains around its coercivity. This is a very important difference that should not be disregarded.

### C. Generic prerequisite for the occurrence of pronounced stray-fields *transverse* magnetic coupling

In this subsection we generalize our experimental findings and we propose a generic *transverse* stray-fields mechanism that may be present in all FM-SC-FM TLs and multilayers. This mechanism is based on a single prerequisite for the occurrence of *transverse* stray-fields magnetic coupling between FM layers that are separated by SC interlayers. We propose that in order an intense MR effect to be observed *the coercive fields of the FM layers should be approximately the same so that the two FM layers should be susceptible to get magnetically coupled*. This condition ensures that in the same field range where the first FM layer exhibits a multidomain magnetic structure that is accompanied by a rich reservoir of *transverse* stray fields all over its surface, also the second FM layer should be divided in magnetic domains so that the stray fields outgoing the first layer will be efficiently

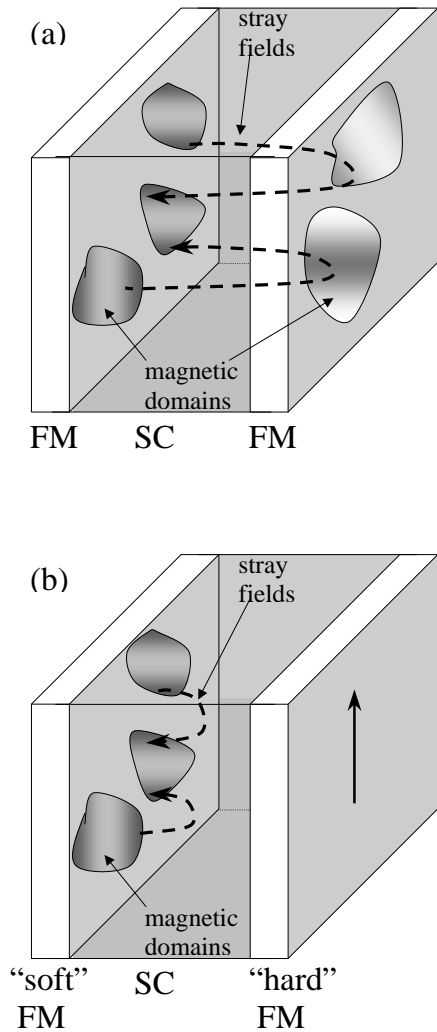


FIG. 7: Schematic representation of (Panel (a)) efficient and (Panel (b)) incomplete stray-fields coupling of two FM layers spaced by a SC interlayer. In the first case the FM layers have almost identical coercive fields, while in the second one their coercive fields are quite different.

sunk in the second one. In the case where the two FM layers don't share almost common coercive fields the effectiveness of *transverse* stray-fields coupling should be minimum. For instance, consider the case where the first FM layer is quite magnetically "soft", while the second one is rather magnetically "hard". Around its coercivity the "soft" FM layer will be accompanied by rich stray fields that since they are randomly distributed will not be effectively delivered to the "hard" FM layer owing to its robust ordered magnetization. This scenario is schematically presented in figure 7. In panel (a) we see that when the respective coercive fields coincide the simultaneous occurrence of magnetic domains in the outer FM layers will ensure their magnetic coupling so that the SC interlayer should be magnetically "pierced", completely. In contrast, in panel (b) we present the case where the re-

spective coercive fields are very different. Thus, complete coupling of the FM layers can't be accomplished so that the SC interlayer may repel the weak *transverse* stray fields that originate from each single FM layer around its coercivity. Consequently, in the first case the transport properties of the SC interlayer are seriously affected, while in the second one only a minor influence occurs.

This proposition explains naturally the occurrence of the pronounced MR peaks that were observed in Refs.9,15,17. In all these works the FM layers participating a TL had almost identical coercive fields as this is evidenced by the only minor two-step behavior observed in the presented  $m(H)$  loops. In contrast, when the coercive field of the first FM layer is significantly different than that of the second one the stray-fields *transverse* magnetic coupling is not intense so that the magnetoresistance effect is getting weak. This is evidenced by the experimental results presented in Refs.6,7,8,10. In Ref.10 the two FM layers exhibit a few tens Oe different coercive fields as this is clear by the distinct two-step behavior in the presented  $m(H)$  loops. Furthermore, in Refs.6,7,8 the coercive fields of the outer FM layers differ by several hundreds Oe. Summarizing these data, compared to the magnetoresistance effect reported in Refs.9,15,17, where the FM layers share almost common coercive fields, the one reported in Ref.10, where distinct coercive fields of the FMs are clearly resolved, is weaker. Eventually, in Refs.6,7,8, where the coercive fields are very different, notable MR peaks were not reported. Thus, it is natural to assume that when the coercive regimes of the two FM layers exhibit significant overlapping the observed MR effect is pronounced, while as the coercivities get progressively different the MR peaks eventually disappear. *We believe that the only mechanism that could be invoked for the consistent interpretation of all these experimental data that are reported in the recent literature<sup>6,7,8,9,10,14,15,17,27</sup> is the stray-fields coupling of the outer FM layers that "pierces" magnetically the SC interlayer.* The specific condition described here should not be restricted only to TLs of SC interlayer but should also hold for TLs having NM and IN interlayers.<sup>1,2,3,4</sup>

#### D. Longitudinal stray fields and the upper-critical field curve of the TL

Finally, in this subsection we discuss the intriguing behavior of the upper-critical field that is observed in the FM-SC-FM TLs for the parallel-field configuration studied in this work. Also, comparative results are presented for a SC-FM BL and a SC SL. Representative raw transport data are shown in figures 8(a)-8(c) for a TL:NiFe19-Nb50-NiFe38, a BL:Nb50-NiFe38, and a SL:Nb50, respectively.

In figures 9(a)-9(b) we present the respective upper-critical field curves  $H_{c2}^{SC}(T)$  for relatively low and high magnetic fields, respectively. The curves of the BL and the SL are shifted in temperature for the sake of the pre-

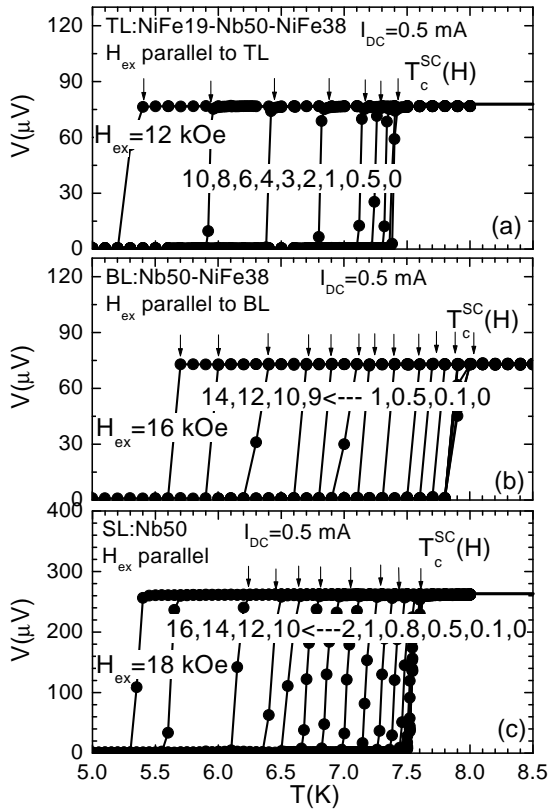


FIG. 8: Representative raw transport  $V(T)$  curves for a TL: NiFe19-Nb50-NiFe38 (Panel (a)), a BL: Nb50-NiFe38 (Panel (b)), and a SL: Nb50 (Panel (c)). In all cases the magnetic field was applied parallel to the films and the current  $I_{dc} = 0.5$  mA was applied normal to the external field.

sentation. These data clearly reveal that the hybrid TL experiences a significant suppression in its upper-critical field curve in the low-field regime when compared to both the BL and the reference Nb SL. In contrast, for magnetic fields exceeding 6 kOe the linear temperature dependence of  $H_{c2}^{SC}(T)$  is recovered.

The experimental data that are presented in figures 9(a)-9(b) show clearly that for the TL the  $H_{c2}^{SC}(T)$  curve experiences an intense crossover from a 2D to 3D behavior at  $(H^*, T^*) = (6 \text{ kOe}, 6.8 \text{ K})$ . It seems that for low magnetic fields and close to  $T_c^{SC}$ , i.e. for  $H < H^*$  and  $T > T^*$  the Nb interlayer behaves as a 2D SC having thickness lower than the coherence length,  $\xi(T)$  of the Cooper pairs.<sup>31</sup> In contrast, for  $H > H^*$  and  $T < T^*$  it behaves as a usual 3D SC film. The respective BL and the Nb SL also exhibit such a crossover but of much lower intensity. In fact the characteristic point  $(H^*, T^*)$  where the crossover is observed is shifted at progressively lower (higher) fields (reduced temperatures,  $T/T_c^{SC}$ ) starting from the TL to the SL.

There is no doubt that for the Nb SL the observed crossover relates exclusively to a thermally driven process that takes place as the temperature dependent coherence length,  $\xi(T) = \xi(0)[1/(1 - T/T_c^{SC})^{1/2}]$  gets

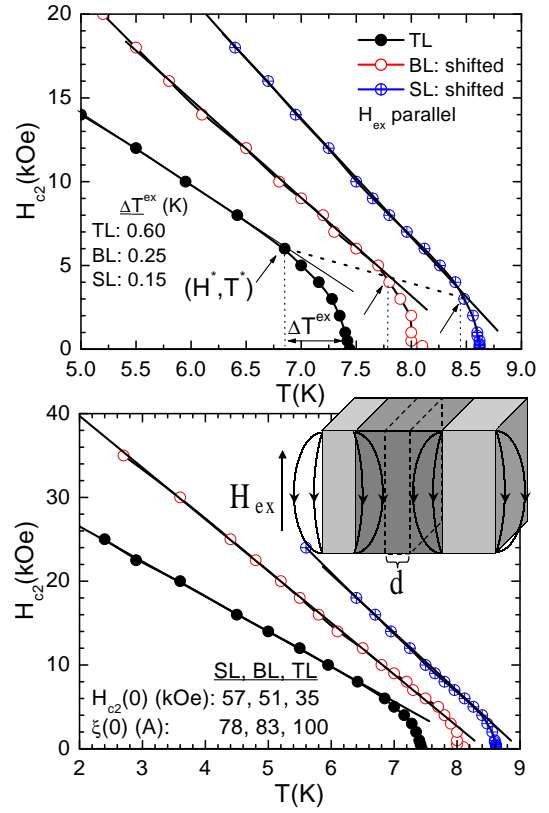


FIG. 9: Upper-critical field curves for a TL: NiFe19-Nb50-NiFe38 (solid circles), a BL: Nb50-NiFe38 (open circles), and a SL: Nb50 (circles with crosses) in the high-temperature, low-field regime (Panel (a)) and in an extended range (Panel (b)). In all cases the magnetic field was applied parallel to the films. The BL's and SL's curves are shifted in temperature for the sake of presentation. The obtained curves change behavior from 2D to 3D at different points  $(H^*, T^*)$  for each specimen. The TL (SL) exhibits the most (least) wide 2D regime. More specifically, at  $(H^*, T^*) = (6 \text{ kOe}, 6.8 \text{ K})$  the  $H_{c2}^{SC}(T)$  curve of the TL changes behavior from 3D ( $H > H^*$  and  $T < T^*$ ) to 2D ( $H < H^*$  and  $T > T^*$ ). The inset presents schematically the outer FM's longitudinal stray fields that penetrate the SC interlayer beside the interfaces. A "stray-fields-free regime" of thickness  $d$  may be formed in the SC's interior (see text for details).

equal to the thickness of the film since it diverges at  $T_c^{SC}$ .<sup>31</sup> Indeed, for the Nb SL the zero-temperature coherence length  $\xi(0)$  as this is estimated from the zero-temperature extrapolation of the  $H_{c2}^{SC}(T)$  curve by using the mean-field theoretical formula  $H_{c2}(T) = \Phi_0/2\pi\xi^2(T)$  is  $\xi(0) \simeq 78 \text{ Å}$  ( $H_{c2}^{SC}(0) \simeq 57 \text{ kOe}$ ).<sup>31</sup> Subsequently, by simulating the temperature variation of the coherence length  $\xi(T) = \xi(0)[1/(1 - T/T_c^{SC})^{1/2}]$  we are able to find the characteristic temperature  $T^*$  where  $\xi(T)$  equals the thickness of the Nb SL. The theoretically estimated temperature width  $\Delta T^{th} = T_c^{SC} - T^*$  where such a 2D behavior should be observed is  $\Delta T^{th} \approx 0.2 \text{ K}$ . This value correlates nicely with the experimental one  $\Delta T^{ex} = 0.15 \text{ K}$ . In the related Table we present all the experimentally



TABLE I: Theoretically estimated and experimentally accessible values of the temperature width  $\Delta T$  where  $2D$  behavior should be observed for samples NiFe19-Nb50-NiFe38 TL, NiFe19-Nb50 BL, and NiFe38 SL. Also, presented are the experimental zero-temperature critical field  $H_{c2}^{SC}(0)$  and coherence length  $\xi(0)$  values that were used for the theoretical estimations. Finally, presented are the values of the characteristic field  $H^*$  where the  $2D$  to  $3D$  crossover is observed for each sample.

	$\Delta T^{th}$ (K)	$\Delta T^{ex}$ (K)	$H_{c2}^{SC}(0)$ (kOe)	$\xi(0)$ (Å)	$H^*$ (kOe)
TL	0.4	0.6	35	100	6
BL	0.3	0.25	51	83	4
SL	0.2	0.15	57	78	3

obtained and the theoretically estimated parameters for all TL, BL and SL.

A number of observations may be extracted from these data. The experimentally determined temperature widths  $\Delta T^{ex}$  exceed significantly the theoretically estimated ones  $\Delta T^{th}$  especially for the TL. In principle both  $\Delta T^{ex}$  and  $\Delta T^{th}$  should depend on the quality of the SC layer since the zero-temperature values of both the upper-critical field  $H_{c2}^{SC}(0)$  and the coherence length  $\xi(0)$  depend on the existing crystal disorder (recall that in the dirty limit the zero-temperature coherence length  $\xi(0)$  is limited by the mean-free path parameter  $l$  since the expression  $\xi(0) \approx \sqrt{l\xi_0}$  holds, where  $\xi_0$  is the BCS coherence length in the clean limit).<sup>31</sup> Thus, a variation of the experimentally observed  $\Delta T^{ex}$  values among different samples should not be paradox. However, in our data we observe a *systematic* evolution of the characteristic point  $(H^*, T^*)$  where the crossover occurs. Moreover, the field dependence of the crossover point as this is evident by the gradual increasing of the  $H^*$  value when an additional FM layer is getting added from the SL to the BL and from the BL to the TL can't be interpreted by the concept of a purely *thermally* driven  $2D$  to  $3D$  process. Instead, we believe that there is a *field* driven process that contributes, significantly.

Below, based on the influence of the *longitudinal* stray fields of the saturated outer FM layers on the SC interlayer we discuss such a possible field driven process. Since the saturation field of the NiFe outer layers is  $H_{sat}^{FM} = 20$  Oe (see inset of figure 1(a)) even in the low field regime,  $H_{sat}^{FM} < H < H^*$  where the rounding of the TL's  $H_{c2}^{SC}(T)$  curve is observed these FM layers are *saturated*. Thus, since magnetic domains don't exist at saturation *transverse* stray fields are not expected; for  $H_{sat}^{FM} < H < H^*$  the stray fields are *longitudinal* since they run along the surfaces of the outer NiFe layers (see the schematic inset of figure 9(b)). These *longitudinal* stray fields penetrate the Nb interlayer at a depth that depends on both the geometric characteristics of the hybrid structure and the magnetic characteristics of the FM layers (for instance, the saturation magnetization determines the intensity of stray fields). However, since the Nb interlayer is quite thick (50 nm) we expect that in its interior there could

exist a regime that is not affected by the *longitudinal* stray fields. This is illustrated in the inset of figure 9(b) as a "stray-fields-free regime" of width  $d$ . Accordingly, for low magnetic fields the influence of the *longitudinal* stray fields should be considered as the most important parameter that acts against superconductivity at least at a depth  $(50 - d)/2$  nm by the FM-SC interfaces. Especially for magnetically "soft" FM materials, as is NiFe in our case, these *longitudinal* stray fields could be quite strong ranging between hundreds Oe to a few kOe. Thus, close to  $T_c^{SC}$  where the effect is observed the  $H_{c2}^{SC}(T)$  attains low values so that the *longitudinal* stray fields could strongly suppress superconductivity at a depth of their range. A key-notice is that the *longitudinal* stray fields are opposite to the external magnetic field,  $H_{ex}$ . Thus, as the externally applied field increases it should gradually compensate the *longitudinal* stray fields due to their opposite orientations. Obviously, the compensation will start from the SC's interior since there the *longitudinal* stray fields are weaker. Consequently, this gradual compensation will expand the "stray-fields-free regime" and  $d$  will increase, eventually getting equal to the Nb interlayer's thickness as the external magnetic field equals the intensity of stray fields. Thus, *in order to explain the 2D to 3D crossover observed in the TL at  $(H^*, T^*) = (6$  kOe, 6.8 K) we speculate that according to the process described above in low magnetic fields,  $H < H^* = 6$  kOe the width  $d$  of the "stray-fields-free regime" is lower than the coherence length  $\xi$  so that the Nb interlayer behaves as a 2D SC, while at some characteristic value of the applied magnetic field  $H^* = 6$  kOe the width  $d$  of the "stray-fields-free regime" will become equal to, and eventually exceed, the coherence length  $\xi$  so that for  $H > H^* = 6$  kOe the Nb interlayer will start to behave as a 3D SC. For the BL where a second outer FM layer is missing this process should be weaker. The "stray-fields-free regime" should be wider for the BL when compared to the TL so that lower applied fields are needed for entering the 3D regime. This is in nice agreement to our experimental findings that are shown in figure 9 and summarized in the related Table. Of course, in order this proposition to be proved definitely, a complete series of TLs where the thickness of the Nb interlayer is systematically varied should be studied. This systematic work is in progress. However, we believe that this draft proposal captures consistently the experimental data already available.*

## VI. CONCLUSIONS

In summary, we demonstrated that TLs comprised of low spin polarized NiFe and low- $T_c$  Nb exhibit special features in both low and high magnetic fields. For low magnetic fields they behave as superconducting switches since they exhibit a two orders of magnitude boost in the MR very close to  $T_c^{SC}$ . Their dynamic transport behavior is revealed through I-V characteristics. The normal state magnetic characterization, but most importantly

the complete evolution of both the *longitudinal* and *transverse* magnetic components from very close to well below  $T_c^{SC}$  are presented. These data show that in the superconducting regime the SC attains a *transverse* magnetic component since it behaves diamagnetically not in respect to the external magnetic field but in respect to *transverse* stray fields that interconnect the outer NiFe layers. Consequently, the pronounced MR effect observed in our TLs is due to the suppression of superconductivity by the *transverse* stray fields related to the domain walls that emerge at coercivity.

A plausible *transverse* stray-fields mechanism is proposed that gives fair explanation for the intense MR effects that are observed in relevant hybrid TLs. This mechanism is based on a single, and probably, generic prerequisite: intense MR effect are observed when the coercive fields of the outer FM layers are almost identical since under this condition the *simultaneous* occurrence of magnetic domains will provide *transverse* stray fields all

over the FMs' surfaces that may mediate effectively their magnetic coupling.

Finally, the upper-critical field curve  $H_{c2}^{SC}(T)$  of hybrid TLs is presented and discussed in comparison to the ones of a BL and a SL reference films. For the TL a pronounced suppression is observed in the low-field regime, while the conventional linear temperature variation is recovered for significantly higher magnetic fields when compared to the BL and the SL. Based on the influence of *longitudinal* stray fields arising from the outer NiFe layers when these are saturated we propose a possible model for the interpretation of this intense  $2D$  to  $3D$  crossover. According to this explanation the respective process should be weaker for the BL. This is in agreement to our experimental results.

*Note:* This work is dedicated to Professor S.H. Papadopoulos who has been a great pedagogue and a sincere humanitarian.

- 
- <sup>1</sup> M.N. Baibich, J.M. Broto, A. Fert, Van Dau F. Nguyen, F. Petro, P. Eitenne, G. Creuzet, A. Friederich, J. Chazelas, Phys. Rev. Lett. 61 (1988) 2472.
- <sup>2</sup> B. Dieny, J. Magn. Magn. Mater. 136 (1994) 335.
- <sup>3</sup> S. Gider, B.U. Runge, A.C. Marley, S.S.P. Parkin, Science 281 (1998) 797.
- <sup>4</sup> L. Thomas, M.G. Samant, S.S.P. Parkin, Phys. Rev. Lett. 84 (2000) 1816.
- <sup>5</sup> M.D. Allsworth, R.A. Chakalov, M.S. Colclough, P. Mikheenko, C.M. Muirhead, Appl. Phys. Lett. 80 (2002) 4196; P. Mikheenko, R.A. Chakalov, R. Chakalova, M.S. Colclough, C.M. Muirhead, Physica C 408-410 (2004) 365.
- <sup>6</sup> J.Y. Gu, C.Y. You, J.S. Jiang, J. Pearson, Ya B. Bazaliy, S.D. Bader, Phys. Rev. Lett. 89 (2002) 267001.
- <sup>7</sup> A. Potenza, C.H. Marrows, Phys. Rev. B 71 (2005) 180503(R).
- <sup>8</sup> I.C. Moraru, W.P. Jr. Pratt, N.O. Birge, Phys. Rev. Lett. 96 (2006) 037004.
- <sup>9</sup> V. Pena, Z. Sefrioui, D. Arias, C. Leon, J. Santamaria, J.L. Martinez, S.G.E. Velthuis, A. Hoffmann, Phys. Rev. Lett. 94 (2005) 57002.
- <sup>10</sup> A.Yu Rusanov, S. Habraken, J. Aarts, Phys. Rev. B 73 (2006) 060505(R).
- <sup>11</sup> D. Stamopoulos, N. Moutis, M. Pissas, D. Niarchos, Phys. Rev. B 72 (2005) 212514.
- <sup>12</sup> D. Stamopoulos, M. Pissas, Phys. Rev. B 73 (2006) 132502.
- <sup>13</sup> D. Stamopoulos, Supercond. Sci. Technol. 19 (2006) 652.
- <sup>14</sup> D. Stamopoulos, E. Manios, M. Pissas, Phys. Rev. B 75 (2007) 014501.
- <sup>15</sup> R. Steiner, P. Ziemann, Phys. Rev. B 74 (2006) 094504.
- <sup>16</sup> A. Singh, C. Sürgers, H.V. Löhneysen, Phys. Rev. B 75 (2007) 024513.
- <sup>17</sup> C. Visani, V. Peña, J. Garcia-Barriocanal, D. Arias, Z. Sefrioui, C. Leon, J. Santamaria, N.M. Nemes, M. Garcia-Hernandez, J.L. Martinez, S.G.E. te Velthuis, A. Hoffmann, Phys. Rev. B 75 (2007) 054501.
- <sup>18</sup> C. Monton, F. de la Cruz, J. Guimpel, Phys. Rev. B 75 (2007) 064508.
- <sup>19</sup> A.F. Volkov, F.S. Bergeret, K.B. Efetov, Phys. Rev. Lett. 90 (2003) 117006; *ibid*, 86 (2001) 4096; *ibid*, Phys. Rev. B 69 (2004) 174504.
- <sup>20</sup> M.Yu. Kharitonov, A.F. Volkov, K.B. Efetov, Phys. Rev. B 73 (2006) 054511.
- <sup>21</sup> T. Lfwander, T. Champel, J. Durst, M. Eschrig, Phys. Rev. Lett. 95 (2005) 187003; M. Eschrig, J. Kopu, J.C. Cuevas, G. Schön, *ibid*, 90 (2003) 137003.
- <sup>22</sup> T. Lfwander, T. Champel, M. Eschrig, Phys. Rev. B 75 (2007) 014512.
- <sup>23</sup> M.A. Maleki, M. Zareyan, Phys. Rev. B 74 (2006) 144512.
- <sup>24</sup> A.I. Buzdin, A.V. Vedyayev, N.V. Ryzhanova, Europhys. Lett. 48 (1999) 686.
- <sup>25</sup> L.R. Tagirov, Phys. Rev. Lett. 83 (1999) 2058.
- <sup>26</sup> S. Takahashi, H. Imamura, S. Maekawa, Phys. Rev. Lett. 82 (1999) 3911.
- <sup>27</sup> D. Stamopoulos, E. Manios, M. Pissas, Phys. Rev. B 75 (2007) 184504.
- <sup>28</sup> D. Stamopoulos, M. Pissas, E. Manios, Phys. Rev. B 71 (2005) 014522.
- <sup>29</sup> D. Stamopoulos, E. Manios, Supercond. Sci. Technol. 18 (2005) 538.
- <sup>30</sup> We note that in agreement to Ref.10 we prefer to use the definition  $(R_{max} - R_{min})/R_{nor} \times 100\%$  (that takes into account the reference resistance value obtained in the normal state) for the description of the underlying physics since the alternative one  $(R_{max} - R_{min})/R_{min} \times 100\%$  (that takes into account the minimum value obtained in the superconducting state) suffers from possible singularities originating from the zeroing of the measured resistance that naturally occurs in every SC (see Fig.2(c)).
- <sup>31</sup> M. Tinkham, *Introduction to Superconductivity* (1996) New York: McGraw-Hill.